

Numerical and Experiment Study of Residual Stress and Strain in Multi-Pass GMA Welding

ReenalRitesh Chand^{1, a}, Ill-Soo Kim^{1, b}, Ji-Hye Lee^{1, c} and Ji-Sun Kim^{2, d}

¹Department of Mechanical Engineering, Mokpo National University, 16, Dorim-ri, Chungkye-myun, Muan-gun, Jeonnam 534-729, South Korea

²Korea Institute of Science and Technology, 971-35 Wolchul-dong, Buk-gu, Gwangju, 50-460 South Korea

^areenal_r@yahoo.com, ^bilsookim@mokpo.ac.kr, ^cjihyelee@mokpo.ac.kr, ^dkimjisun@kitech.re.kr

Keywords: Finite Element Method, Residual Stress, Strain, GMA welding

Abstract. There must be selection of an optimal welding parameter and condition that reduces the risk of mechanical failures on weld structures. The residual stress and welding deformation have a large impact on the failure of welded structures. To achieve the required precision for welded structures, it is required to predict the welding distortions at the early stages. Therefore, this study uses the 2D Finite Element Method (FEM) to predict residual stress and strain on thick SS400 steel metal plate. A birth and death technique is employed to control the each weld pass welding. Gas Metal Arc (GMA) welding experiment is also performed with similar welding condition to validate the FE results. The simulated and experiment results provide good evidence that heat input is mainly dependent on the welding parameter and residual stress and distortions are mainly affected by amount of heat input during each weld-pass.

Introduction

Automated GMA welding is currently one of the most popular welding methods, especially in a broad range of industrial environments such as in areas of renewable energy. In GMA welding, heat source is created by an arc and maintained between a consumable electrode wire and work-piece. The weld is formed by melting and solidification of the filler material and base material. Inert gas is allowed to flow during the welding process to shield the weld metals from the surrounding atmosphere [1-6].

The local, non-uniform heating and subsequent cooling during the multi-pass welding process causes complex thermal stress/strain field to develop that finally leads to residual stress, distortion. The mechanical characteristics such as residual stress, distortion are prime concern to the industries producing weld-integrated structures around the world due to its obvious potential to cause inaccuracy in final welded structures [1]. Residual stress, developed in and around the welding zone are detrimental to the integrity and the service behavior of welded structures. During the welding process, the weld area is heated up sharply compared to the surrounding area and fused locally. The material expands as a result of being heated [2]. The heat expansion is restrained by the surrounding cooler area, which gives rise to thermal stresses. To predict the magnitude and trends of residual stress and deformation fields is a complex phenomenon due to the involvement of various factors including short term localized heating and rapid cooling and metallurgical transformations [3]. Therefore, the FE based numerical simulations attained a considerable importance for the prediction of adverse consequences of complex multi-pass welding.

In this study, a two-dimensional finite element model was developed to predict the residual stress and deformation in multi-pass GMA welding process. The developed model employs Goldak's heat distribution, to simulate welding on SS400 steel butt-weld joint with a thickness of 16mm. Furthermore, FE results are validated with multi-pass experiment with similar welding condition as FE analysis.

Development of welding Simulation model

The GMA welding process is a coupled thermo-mechanical phenomenon is employed to evaluate the residual stress and deformations. Thus this coupled welding phenomenon can be split into thermal analysis followed by structural analysis.

Heat source modeling

The evolution thermal analysis is quite a complex phenomenon associated with GMA welding process. The weld pool shape can be largely influenced by the weld metal transfer mode and corresponding fluid flow dynamics [9]. In representation of GMA welding, the most widely acceptable double heat source model presented by Goldaks et al.[11] being used for the FE modeling as shown in Fig. 1.

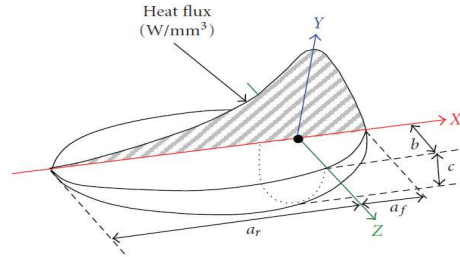


Fig.1 Goldak's double ellipsoid heat source model[9].

The models give the Gaussian distribution for the butt and have excellent features of power and density distribution control in weld pool and HAZ. The Goldak's heat distributions are expressed by the following equations [10]:

$$q(x, y, z) = \frac{\sqrt[6]{3c} Q_w}{abc\pi\sqrt{\pi}} e^{-3x^2/a^2} e^{-3y^2/b^2} e^{-3z^2/c^2} \quad (1)$$

The parameter of moving heat source has been chosen to compute melted zone of thermal simulation and welding process parameter are listed in Table1 and 2. In this simulation the each pass process parameter is different. The contribution of the transient temperature field is also temperature-dependent thermo-physical properties as shown in Fig. 2. Heat conduction problem has been solved using heat transfer analysis to obtain temperature histories. The combined heat transfer coefficient is expressed as follows;

$$h = 24.1 \times 10^{-4} \varepsilon T^{1.61} \quad (2)$$

where ε is emissivity of the surface of the body, a value of 0.9 is assumed for this study[9].

Table 1: Parameter of double ellipsoidal heat source.

Weld pass	a(mm)	b(mm)	c _f (mm)	c _r (mm)	f _f	f _r
1	4.5	4.5	6	16	0.5454	1.4545
2	9	9	6	12.2	0.6593	1.3407
3	7	7	6	25	0.3870	1.6129
4	8.2	10	10.4	13.3	0.8776	1.1224
5	9.3	9.8	7.4	14.8	0.667	1.3333

Table 2: Welding process parameters

Weld pass	Welding Voltage(V)	Arc Current (A)	Welding speed (mm/min)
1	23	200	11
2	26	280	
3	25	240	
4	25	260	
5	20	230	

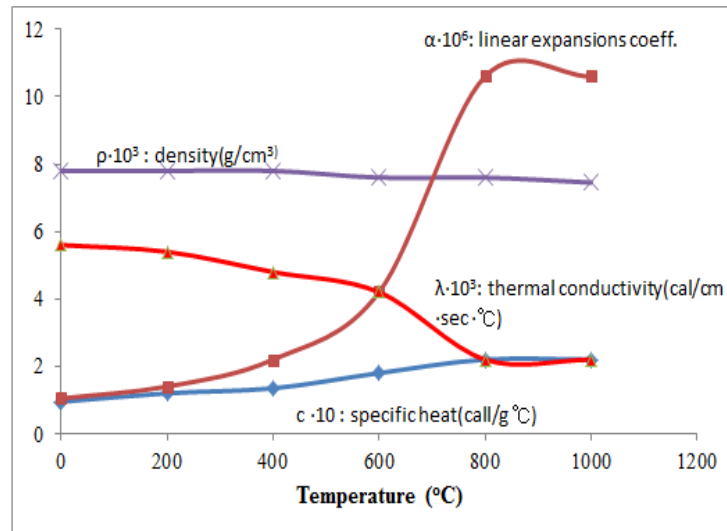


Fig. 2 Thermo-physical properties of SS400 steel as a function of temperature.

The 2D thermal FE computational procedures has been developed to calculate the temperature histories for 5 bead multi-pass GMA welding process at different cooling time of SS400 steel. The dimension for five-pass finite element model is the 400mm in length and 16mm in thickness as shown in Fig. 3.

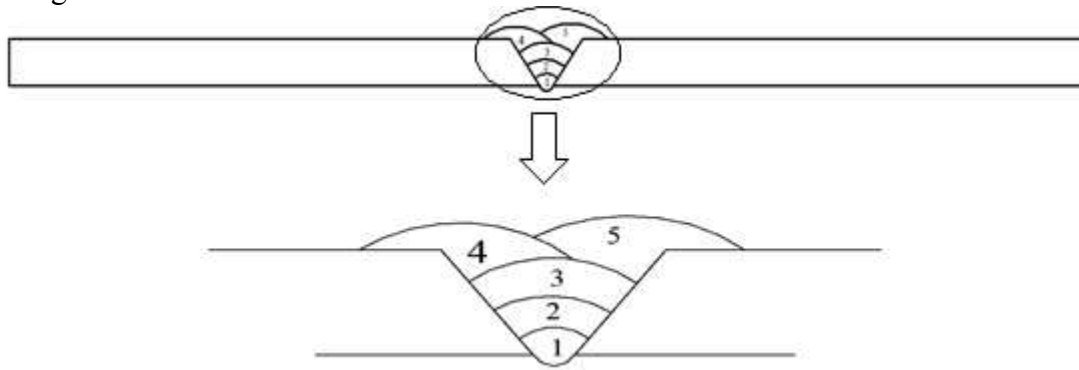


Fig. 2 Dimensional details and weld bead sequence for 5 pass butt weld.

Structural Analysis

For mechanical analysis, the temperature history of each node from the preceding thermal analysis is input as the node load with temperature dependent mechanical properties shown in Fig. 4. The von mises yield criteria is employed with σ_1 , σ_2 , and σ_3 being the three principal stresses, coupled to a kinematic hardening rule,

$$\sigma_v = \sqrt{\frac{1}{2} \left[(\sigma_1 - \sigma_2)^2 + (\sigma_2 - \sigma_3)^2 + (\sigma_3 - \sigma_1)^2 \right]} \quad (3)$$

The total strain can therefore be decomposed into three components as follows:

$$\epsilon^{total} = \epsilon^e + \epsilon^p + \epsilon^{th} \quad (4)$$

The component on the right-hand side of above equation corresponds to elastic, plastic and thermal strain, respectively.

The elastic strain is modeled using the isotropic Hooke's law with temperature-dependent Young's modulus and Poisson's ratio. For the plastic strain component, a plastic model is employed with the following features: the Von Mises yield surface and temperature-dependent mechanical properties.

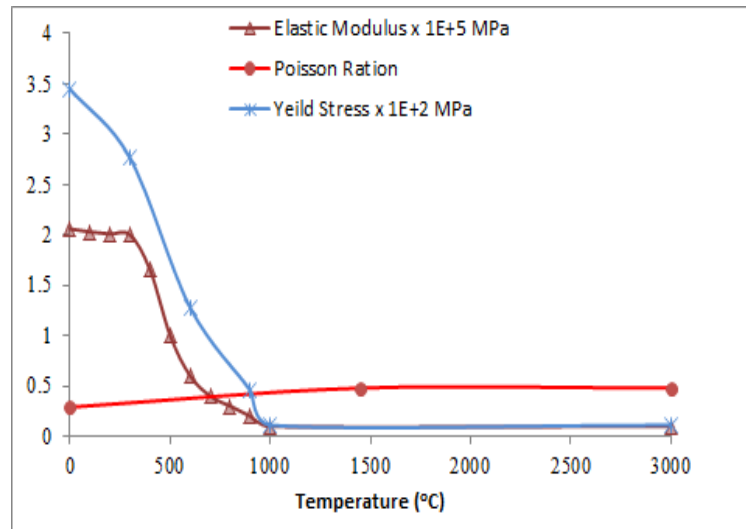


Fig. 4 Thermo-mechanical properties of SS400 steel as a function of temperature.

Experimental Procedure

To validate the FE model, a GMA welding experiment is conducted on 400×200×16 mm thick SS400 steel with similar geometry and welding process parameters from the FE model as shown in Fig. 5. Commercial high-tech, fully automatic GMA M500S welding equipment along with automated wire feeder and welding fixtures were used to reflect the desired structural boundary conditions. Five pass butt-weld geometry is used with single "V" groove having included angle of and 5mm root opening same as FE model as indicated in Fig. 2. The welding carriage is moved with a constant welding speed along the rails.

A non-destructive, x-ray diffraction measurement methods is used to measure residual stress across the welded plate. It uses the interatomic spacing as the ultimate gage length, the X-ray technique is ideal for and applicable to all crystalline materials, especially for metals, but also for ceramics. In addition to the FE parameters, carbon dioxide was used as shielding gas with flow rate of 20 liter/min.

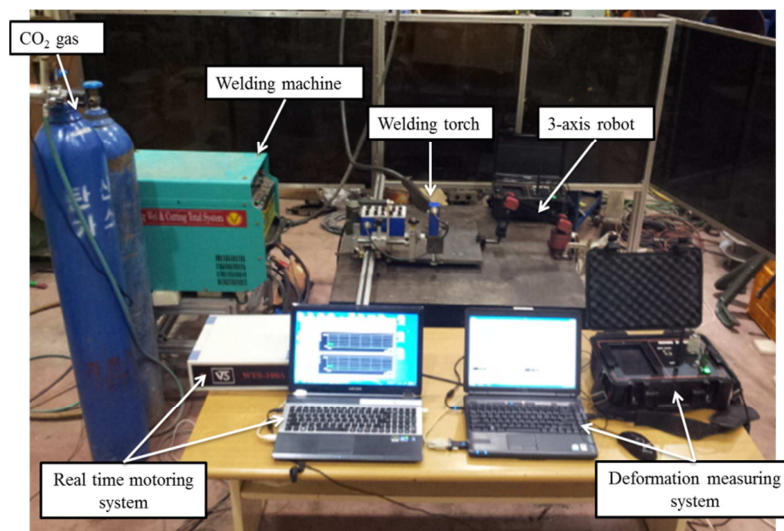
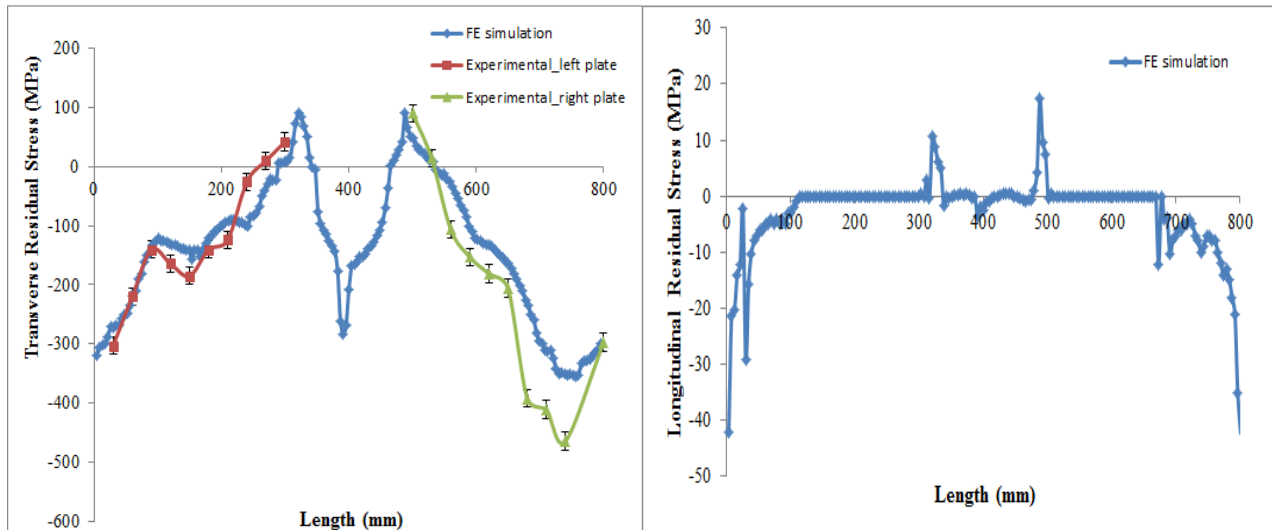


Fig. 5 Multi-pass GMA welding experiment setup.

Results and Discussion

Repeated heating and subsequent cooling has a large impact on the residual stress of the base material during multi-pass welding process material. Tensile and compressive residual stress fields are observed near the weld region based on different temperature distribution on the plate. The different temperature gradient results at the top surface and bottom surface produce different tensile and

compressive residual stress and varying the shrinkage patterns through the thickness of the butt welded plate. The transverse and longitudinal stress distribution along the width at the top surface of the plate is shown in Fig. 6(a) and (b). Fig. 6(a) compares the FE simulation and experimental transverse residual stress, a similar pattern and transverse residual stress and experimental measured residual but there is quite difference in magnitude of the stress. From FE simulation results, it can be observed that around HAZ a tensile stress while at FZ and actual welding region is under compressive residual stress.



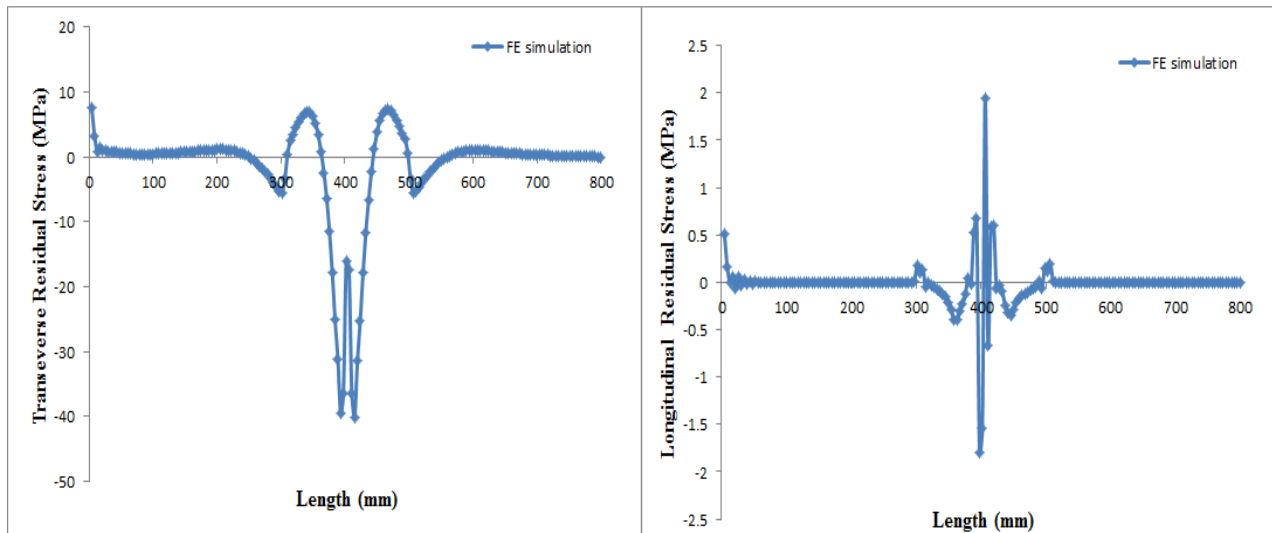
(a) Transverse residual stress

(b) Longitudinal residual stress

Fig. 6 Transverse and Longitudinal residual stress at the top surface of the weld plate.

The edge of the plate and at welding region, a compressive longitudinal residual stress is observed whereas at the HAZ the tensile residual stress. In FZ the stress fluctuate from compressive to tensile stress on the left side of the plate. The residual stress magnitude and distribution at the bottom surface is different compared to top surface due to the groove joint and also weld pass 3, 4 and 5 has large impact on top surface. The transverse residual stress at HAZ is observed to compressive initially but as moved further toward welding region the stress becomes tensile. The large compressive stress is noted at the weld region and FZ as shown in Fig. 7(a). Fig. 7(b) shows longitudinal residual stress at the bottom surface to butt welded plate. At HAZ and FZ the compressive stress and tensile stress is observed.

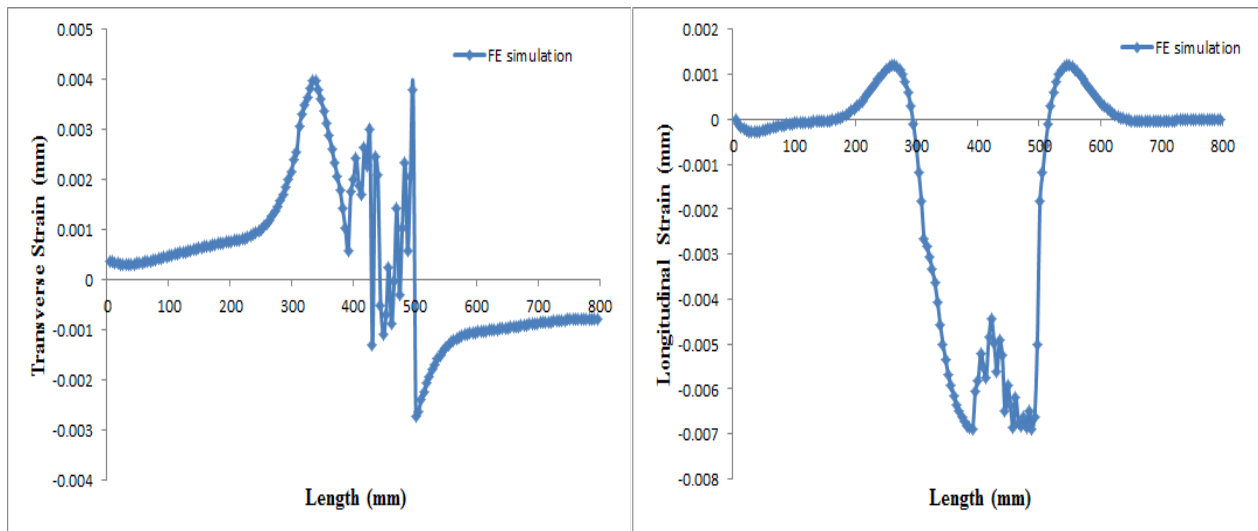
Fig. 8 (a) shows the transverse strain distribution on the plate. It can be observed that the transverse strain distribution at HAZ and FZ is mainly concentrated as tensile strain on the left side plate and at the welding region the strains fluctuate from tensile to compressive. Fig. 8(b) also shows that strain at right side plate are under compressive. The elastic strain at left and right side plate varies due to left side plate being restrained and due to difference in heat load which is applied to the four and five weld-pass. For longitudinal strain, it is observed that the top surface of the plate, have tensile strain at HAZ, whereas at FZ and in vicinity of welding region it has compressive strain.



(a) Transverse residual stress

(b) Longitudinal residual stress

Fig. 7 Transverse and Longitudinal residual stress at the bottom surface of the weld plate.



(a) Transverse strain

(b) Longitudinal strain

Fig. 8 Transverse and longitudinal strain distribution on the welded plate.

Conclusion

2D FE simulations of five pass GMA welding was performed on the 16mm thick SS400 material, to determine residual stress, strain and deflection on the plate. The FE simulation results are verified by experimental results with similar weld conditions and geometry. According to the numerical and experimental analysis results, the following conclusion can be drawn.

- (1) Based on the simulation results, The heat input and peak temperatures of weld pool are depend on the welding process parameter, voltage and current and travelling speed of welding touch, whereas temperature distribution, residual stress and deformation are dependent thermal material properties, heat input, the cooling rate and restrains on the plate.
- (2) It is know that residual stress and strain distribution on top and bottom surface of the plate differs, due to heat distribution load applied to plate, the heat input and also the cooling time after each welding pass. The restraint of plate has also impact on residual stress and strain. The FEM results have much resemblance with the experimental residual stress pattern and magnitude.

References

- [1] C. Heinze, C.Schwenk and M.Rethmeier:Materials and Design, Vol 35, 201-209, 2012.
- [2] D. Deng: Materials and Design, 30 2, February, 359-366, 2009.
- [3] D. Deng and H.Murakawa: Computational Materials Science, 43, August, 353-365, 2008.
- [4] D. Gery, H. Long, and P.Maropoulos,: Journal of Materials Processing Technology, 167, 393-401, 2005.
- [5] D. Deng, W. Liang, and H.Murakawa: Journal of Materials Processing Technology 2007; 183, 2-3: 219-225.
- [6] E. M.Qureshi, A. M. Malik and N. U.Dar: International Journal of Advances in Mechanical Engineering, 2009.
- [7] C. Liu, J.X. Zhang, and C.B.Xue,: Journal of Fusion Engineering and Design, 86, 288-295, 2011
- [8] I.Sattari-Far, and Y.Javadi,:International Journal of Pressure Vessels and Piping, 85(4), April, 265-274, 2008.
- [9] J. A. Goldak and M.Akhlaghi: Computational welding Mechanics Springer, 2005
- [10] J.Goldak, M.Bibby, J.Moore, R. House, B. Patel: Metallurgical Transactions B, 17B(3), p.587-600, 1986.
- [11] J.Goldak, A. Chakravarti and M.Bibby: Int. J. Metallurgical and Materials Transactions B Vol. 15, No. 2, pp. 299–305, 1984
- [12] P. Duranton, J.Devaux, V.Robin, P. Gilles and J.M.Bergheau: J. Materials Pro. Tech.,Vol. 153-154, pp.457-463, 2004.